

MOETION: Efficient and Reliable Sparse Checkpointing for Mixture-of-Experts Models at Scale

Swapnil Gandhi
gandhis@stanford.edu
Stanford University

Christos Kozyrakis
kozyraki@stanford.edu
Stanford University

Abstract

As large language models continue to scale, training them requires thousands of GPUs over prolonged durations—making frequent failures an inevitable reality. While checkpointing remains the primary fault-tolerance mechanism, existing methods struggle to efficiently support Mixture-of-Experts (MoE) models. Due to the substantially larger training state of MoE models, traditional checkpointing techniques incur prohibitive overheads, resulting in frequent stalls or prolonged recovery periods that severely degrade training efficiency.

We introduce MoEtion, a distributed, in-memory checkpointing system designed explicitly for MoE models. MoEtion builds on three key ideas: (1) *sparse checkpointing*, which incrementally checkpoints subsets of experts over multiple iterations, significantly reducing snapshot overhead; (2) a *sparse-to-dense checkpoint conversion* technique that incrementally reconstructs temporally consistent checkpoints from sparse snapshots; and (3) *lightweight upstream logging* activations and gradients at pipeline-stage boundaries to localize recovery of failed workers without redundant recomputation of unaffected workers. Evaluations across diverse MoE models with up to 64 experts demonstrate that MoEtion reduces checkpointing overhead by up to $4\times$ and recovery overhead by up to $31\times$ compared to state-of-the-art approaches, achieving consistently high Effective Training Time Ratios (ETTR) of up to 0.98, even under frequent failures (MTBF as low as 20 minutes) without compromising synchronous training semantics. Overall, MoEtion offers a practical, scalable, and robust fault-tolerance solution for the next generation of sparsely activated models.

1 Introduction

The rise of large foundation models has driven significant scaling in distributed training infrastructure [4, 21, 43, 52, 57–59, 73]. Training state-of-the-art models, such as DeepSeek-V3 with 671B parameters trained on 14.8 trillion tokens [45], requires thousands of GPUs over extended periods, often spanning weeks or even months [1, 3, 29, 36, 40, 53, 62]. At these scales, system failures—triggered by hardware faults, network disruptions, or software bugs—shift from being rare anomalies to frequent events. Major organizations including Microsoft, ByteDance, Alibaba, Google, and Meta have already reported

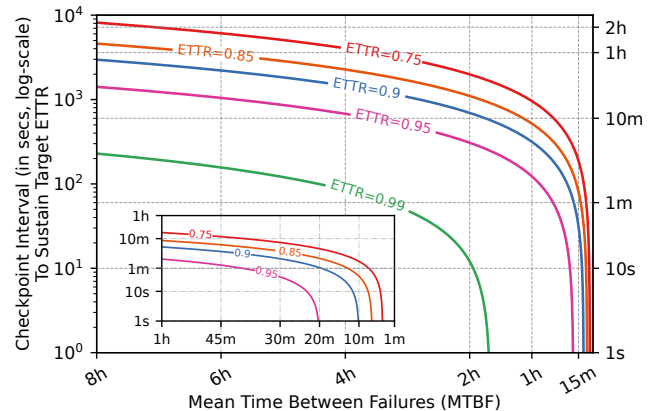


Figure 1: Checkpoint interval required to sustain target ETTR under varying system-wide MTBFs. Contour lines show the upper bound on checkpoint interval for maintaining target ETTR values using the canonical Young/Daly formulation [12, 71]. As system scale increases and MTBF drops—a common scenario in large-scale training—maintaining high training efficiency requires increasingly short checkpoint intervals—highlighting the need for frequent checkpointing in modern systems.

failures as frequently as once every 45 minutes in large-scale training clusters, with the mean time between failures (MTBF) sharply decreasing as GPU count rises [22, 27, 36, 38, 75]. Meta projects an MTBF as low as 14 minutes for jobs utilizing 131,072 GPUs [38], underscoring an emerging reality: *at scale, failure is no longer an anomaly—it is the norm.*

Checkpointing—periodically capturing snapshots of model and optimizer states and persisting them durably—is the standard fault-tolerance mechanism to limit computational loss from failures [1, 3, 9, 21, 22, 27, 36]. To minimize checkpoint overhead, recent techniques leverage overlapping snapshot operations with computation [47, 50, 65], high-performance interconnects [63, 66, 68], checkpoint compression via quantization [2, 16, 46], and redundancy across data-parallel nodes [23]. However, these approaches primarily target dense models, where parameters uniformly contribute to both computation and convergence.

In contrast, Mixture-of-Experts (MoE) models represent a fundamentally different paradigm—replacing dense layers with tens to hundreds (occasionally millions [28]) of sparsely

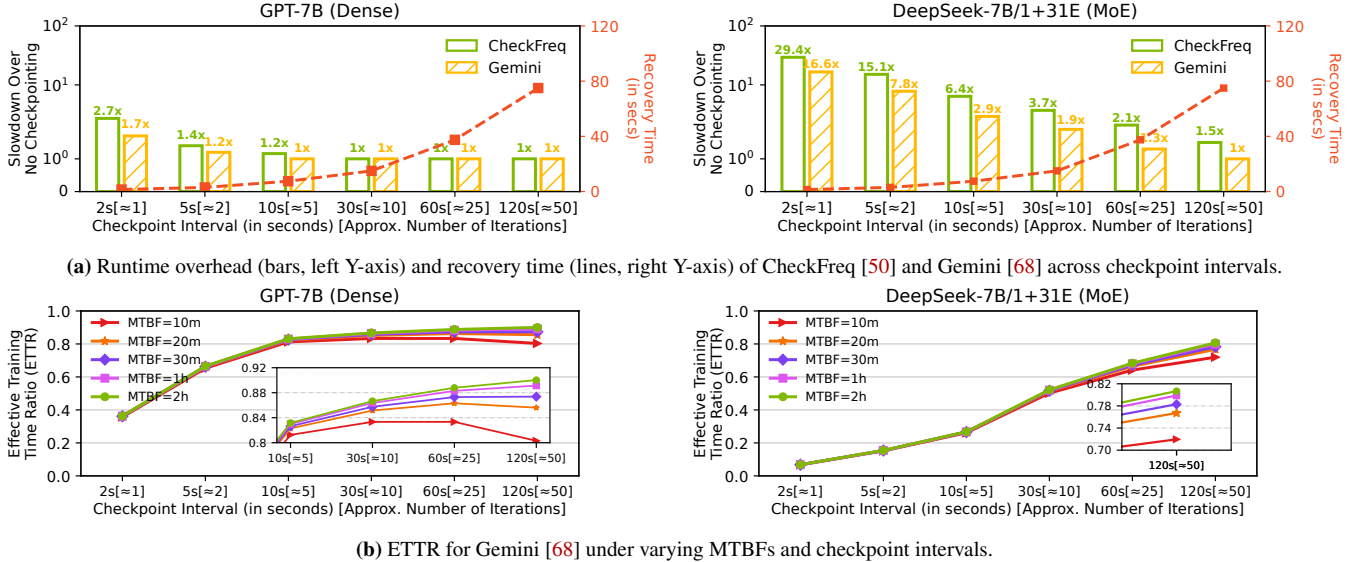


Figure 2: Performance of CheckFreq [50] and Gemini [68] for GPT-7B [6] and DeepSeek-V3-7B/1+31E [11] using 32 A100 GPUs.

activated expert operators [11, 15, 17, 35]. Each input token activates only a small number of experts (typically top-1 or top-2 [7]), enabling an order of magnitude larger parameter counts without proportional increases in computation [39, 41]. Unfortunately, this sparse and dynamically varying operator activation pattern poses significant challenges for traditional checkpointing techniques. Specifically, existing approaches encounter three core challenges with MoE models:

Challenge #1: Runtime–Recovery Tradeoff: State-of-the-art dense checkpointing techniques—such as CheckFreq [50], which pipelines *snapshot* (copying checkpoint state to local CPU memory) and *persist* (flushing the checkpoint to durable storage) phases, and Gemini [68], which employs high-bandwidth remote CPU memory to overlap checkpointing with training—rely heavily on overlapping snapshot I/O with ongoing computation. While effective for dense models, these strategies falter when adapted to MoE models, which typically expand model size by an order of magnitude compared to dense models while maintaining similar iteration times. Consequently, frequent checkpointing imposes substantial runtime overhead. As illustrated in Figure 2a, checkpointing every iteration for DeepSeek-V3-2.4B/1+7E results in runtime slowdowns of 27.4× (CheckFreq) and 9.3× (Gemini). Extending checkpoint intervals alleviates overhead but drastically increases recomputation during recovery, severely limiting the Effective Training Time Ratio (ETTR)¹. Figure 2b shows Gemini achieves an ETTR of merely 0.82 at an MTBF of 2 hours, dropping below 0.75 for projected MTBFs for large-scale scenarios (10–20 minutes).

MoEtion overcomes this limitation by introducing *sparse checkpointing* (§3.2). Rather than checkpointing the entire

model state simultaneously, MoEtion incrementally snapshots subsets of operators across multiple iterations, spreading checkpoint overhead evenly. Operators are strategically grouped based on their activation frequency—less frequently activated (“less popular”) operators are checkpointed earlier, allowing more popular operators to remain in a lightweight frozen state longer, thus significantly reducing recovery overhead (§3.5). This incremental approach fully overlaps checkpoint operations with ongoing computation, enabling frequent, continuous, stall-free checkpointing. As a result, MoEtion effectively eliminates the runtime–recovery tradeoff and consistently maintains high ETTR (≥ 0.9), even at low MTBFs.

Challenge #2: Correctness vs. Efficiency: Recent MoE-specific checkpointing approaches, like MoC-System [8], attempt to reduce checkpoint overhead by checkpointing only a subset of experts per iteration in a round-robin fashion. While temporarily lowering runtime overhead, this strategy compromises correctness: during recovery, experts without recent checkpoints revert to stale states, causing token loss and violating synchronous training semantics [48].

MoEtion addresses this correctness–efficiency tension through a novel *sparse-to-dense checkpoint conversion* mechanism (§3.3). Sparse checkpoints store subsets of operators’ FP32 optimizer states and parameters alongside lightweight FP16 parameters for remaining operators. Upon recovery, MoEtion selectively freezes operators without recent checkpoints, replaying computations incrementally using stored FP16 parameters until all operators achieve fully synchronized dense checkpoint states. This ensures no tokens or training progress are lost during recovery, preserving synchronous training semantics, model accuracy, and reproducibility—without high overheads for fault-free execution.

¹Effective Training Time Ratio measures the fraction of total wall-clock time spent on useful training computations

Challenge #3: Global Rollback Scope: Existing checkpointing methods typically force all GPU workers—both faulty and fault-free—to revert to the same global checkpoint upon a failure [23, 50, 63, 65, 68] to guarantee synchronous semantics, introducing significant recomputation overhead and delaying recovery. Such global rollback exacerbates recovery costs, particularly when checkpointing intervals are extended to reduce runtime overhead.

MoEtion introduces *localized rollback* (§4), a targeted recovery strategy designed to significantly reduce recomputation overhead upon failures. It achieves this by logging intermediate activations and gradients at each pipeline stage boundary (§3.4). When a failure occurs, only the affected data-parallel group rolls back to its most recent sparse checkpoint—typically spanning just a few iterations due to MoEtion’s frequent, stall-free snapshotting—and recovers by locally replaying computations using the stored activation and gradient logs. Consequently, recomputation overhead is limited exclusively to the impacted workers, dramatically accelerating recovery, particularly in large-scale deployments where failures usually affect only a small subset of the cluster.

We implemented MoEtion atop DeepSpeed [59] and evaluated it comprehensively across diverse MoE models spanning both vision and language domains. Our results show that MoEtion significantly improves both checkpointing overhead and recovery efficiency: it reduces checkpointing overhead by up to 4× compared to MoC-System [8], and accelerates recovery by up to 31× and 17× relative to CheckFreq [50] and Gemini [68], respectively. Consequently, MoEtion consistently maintains high Effective Training Time Ratios (ETTRs) ranging between 0.956 and 0.981, even under frequent failure conditions (MTBF as low as 20 minutes). Crucially, these efficiency gains are achieved without compromising model accuracy or incurring noticeable runtime overhead during fault-free training. By effectively addressing the runtime–recovery tradeoff, resolving correctness–efficiency tensions inherent in prior checkpointing methods, and eliminating unnecessary global rollbacks, MoEtion offers a robust and scalable fault-tolerance solution uniquely suited to the demands of large-scale MoE training.

2 Background & Related Work

2.1 Sparse Mixture-of-Experts (MoE) Models

Mixture-of-Experts (MoE) models have emerged as a scalable, compute-efficient design for training large models across various domains. By activating only a subset of their parameters for each input, MoEs significantly increase model size while maintaining low per-token computational costs. This conditional computation paradigm underpins numerous state-of-the-art foundation models, including Gemini [19], DeepSeek-V3 [45], Nemotron [24], LLaMA 4 [49], and DBRX [13].

MoEs extend standard transformers by replacing dense feed-forward layers with multiple parallel subnetworks, or

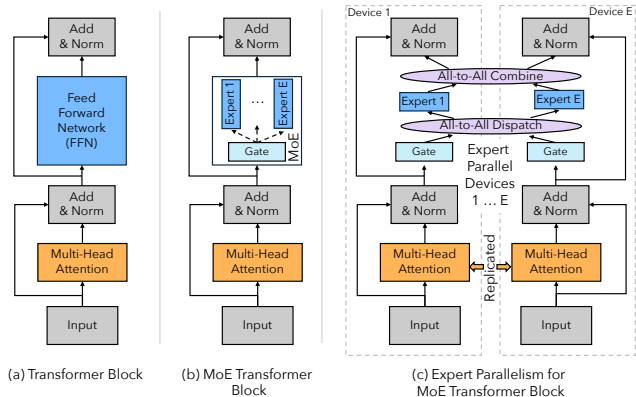


Figure 3: MoE architecture and Expert parallelism.

experts. A learned gating network selects a small number of experts—typically top-1 or top-2—for each token. The outputs from these selected experts are combined through learned weights. This selective activation enables models to scale total parameter counts with only sub-linear growth in computational overhead.

To mitigate expert overuse, MoEs commonly use auxiliary load-balancing objectives [17, 55, 74] to encourage more uniform expert utilization. In practice, however, activation remains naturally skewed due to input diversity, expert specialization, and training dynamics [25, 26, 72]. Attempts at strict balancing through strong regularization can disrupt expert specialization and degrade model performance [17, 45].

2.2 Distributed Training of MoE Models

State-of-the-art MoE models contain hundreds of billions of parameters trained on datasets with trillions of tokens [3, 17, 29, 61]. Training typically spans weeks and requires thousands of GPUs [4, 36, 49]. For instance, DeepSeek-V3, a 671B-parameter model, trained on 14.8 trillion tokens, consumed 2.7 million Nvidia H800 GPU hours—equivalent to 11 days on a 10,000-GPU cluster [45].

MoE training employs four primary parallelism strategies. *Data parallelism* (DP) splits batches across GPUs, synchronizing parameters with all-reduce operations [20, 60]. *Tensor parallelism* (TP) partitions model layers across GPUs to accelerate large matrix operations (e.g., GEMMs) [61]. *Pipeline parallelism* (PP) divides the model sequentially, processing micro-batches in a pipelined fashion [31, 37, 42, 51]. *Expert parallelism* (EP), unique to MoEs, distributes experts across GPUs and routes tokens using all-to-all communication, enabling scalable conditional computation [25, 32, 41, 72].

Frequent Failures in Distributed Training. Modern training clusters comprise thousands of GPUs interconnected by sophisticated networking, storage, and power systems. Meta’s AI Research SuperCluster, for example, integrates over 16,000 GPUs with high-bandwidth InfiniBand interconnects [38]. At this scale and duration, failures are inevitable, arising from hardware faults (e.g., overheating GPUs, SSD degradation),

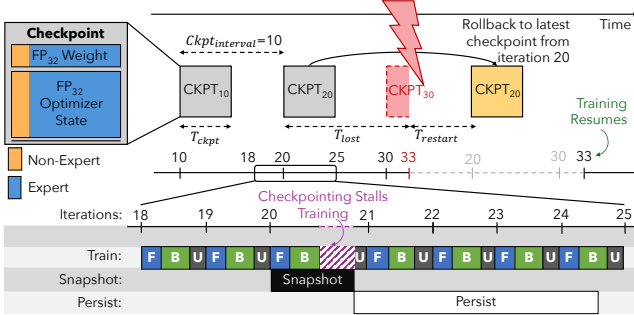


Figure 4: Checkpoint-based fault tolerance in distributed training. A checkpoint is taken every $Ckpt_{interval} = 10$ iterations. On failure, training rolls back to the most recent complete checkpoint (CKPT₂₀) and recomputes lost training progress.

transient network disruptions, software crashes, or service-level issues (e.g., monitoring agents exceeding resource limits) [30, 36, 75]. Alibaba Cloud reported abnormal termination rates of 44% for the top 5% resource-intensive jobs, slowing training by up to 40% [27, 46]. Microsoft observed job-level failures approximately every 45 minutes in a 75-day study of 96,000 jobs [34]. Meta projects MTBF as low as 14 minutes for 130,000-GPU clusters [38], a trend echoed by ByteDance [36], LAION [5], and Google [75].

Unlike loosely coupled frameworks like MapReduce [14], distributed training is tightly synchronized and gang-scheduled. A single node failure typically stalls or crashes the entire job, forcing rollback to the most recent checkpoint.

2.3 Periodic Checkpointing for Fault-Tolerant Training

Distributed training systems recover from failures by resuming from periodically saved checkpoints that encapsulate the full training state—model parameters, optimizer states, and metadata such as iteration counters and RNG seeds [5, 27, 34, 36, 40, 59, 65, 67, 75]. As shown in Figure 4, the majority of checkpoint size is dominated by optimizer state from the expert layers (74%), followed by expert model parameters (12%), non-expert optimizer state (12%), non-expert parameters (2%), and a small fraction of metadata ($\leq 1\%$). Since this state is updated every iteration, training must pause unless the checkpointing operation can be fully overlapped with the next iteration. While increasing the checkpoint interval $Ckpt_{interval}$ enables more overlap, doing so naively can significantly increase recovery time $T_{recovery}$, which is the sum of lost progress that must be recomputed T_{lost} and restart time $T_{restart}$.

2.4 Checkpointing Techniques

Checkpointing for Fault-Tolerant Training. Periodic checkpointing remains the predominant method for achieving fault tolerance in distributed training [27, 34, 36, 40, 59, 65, 67]. However, naive checkpointing introduces significant stalls, severely limiting the Effective Training Time Ratio (ETTR), particularly for large models. Recent methods like Check-

System	Stall Free	Low Overhead High Frequency	Fast Recovery	Full Recovery	High ETTR
CheckFreq [50]	✗	✗	✗	✓	✗
Gemini [68]	✗	✗	✓	✓	✗
MoC-System [8]	✗	✗	✓	✗	✗
MoEtion	✓	✓	✓	✓	✓

Table 1: Comparison of periodic checkpointing techniques.

Freq [50] and Gemini [68] mitigate this overhead by strategically overlapping checkpoint operations with ongoing computation. CheckFreq introduces a two-phase checkpointing pipeline, dynamically adapting checkpoint intervals based on runtime measurements to balance overhead against recovery costs. Gemini employs in-memory checkpointing, utilizing high-bandwidth CPU memory and strategic placement of checkpoints to speed up recovery. Despite these optimizations, both methods incur substantial runtime overhead when frequently checkpointing large MoE models due to their significantly increased checkpoint sizes, as illustrated in Figure 2a. Consequently, neither CheckFreq nor Gemini can fully overlap large MoE checkpoint snapshots with computation, resulting in frequent training stalls and persistently low ETTR—thus failing to adequately address the runtime–recovery tradeoff (Challenge #1).

More recently, MoC-System [8] proposed Partial Expert Checkpointing (PEC) specifically for MoE models. PEC reduces checkpoint size by checkpointing only a subset of experts at each interval, cycling through them in a round-robin fashion. While initially effective in reducing checkpoint overhead, PEC inherently compromises correctness during recovery: experts lacking recent checkpoints revert to stale states, causing token loss and breaking synchronous training semantics. Although MoC-System attempts to mitigate accuracy degradation by adaptively increasing the number of experts checkpointed after each failure, this approach rapidly devolves into dense checkpointing under frequent failures, nullifying its initial efficiency advantage. As a result, MoC-System struggles to balance correctness and efficiency (Challenge #2).

Other checkpointing optimizations include storage-level enhancements such as NVMe-driven checkpoint acceleration (Fast-Persist [66]), concurrent data-parallel checkpoint sharing (Megascale [36]) and persistence (PCCheck [63]), parallelism-agnostic checkpoint representations (ByteCheckpoint [65]), and checkpoint size reduction via model-specific quantization (Check-N-Run [16], CPR [46]). Yet, these techniques still require checkpointing the entire model state simultaneously, inevitably causing stalls and limiting achievable checkpoint frequency.

Checkpoint-less Fault-Tolerance. An orthogonal approach to traditional checkpointing involves exploiting redundancy within training setups to minimize or eliminate periodic checkpoints entirely. Just-in-Time [23] exploits redundancy across data-parallel replicas, deferring checkpointing until failures are actually detected. More aggressive checkpoint-less strategies include Bamboo [64], which introduces redundant com-

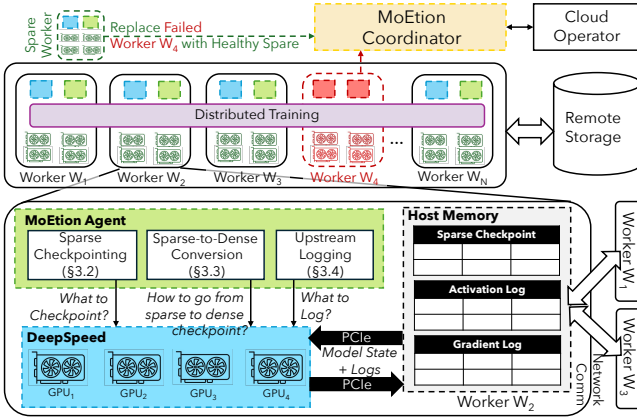


Figure 5: The system architecture of MOETION

putations to withstand preemptions in cloud spot instances, Ooblock [33], which utilizes heterogeneous pipelines to recover efficiently from failures without requiring spare resources, and ReCycle [18], which dynamically reroutes workloads to functionally redundant data-parallel peers to continue computation seamlessly after failures.

However, these checkpoint-less methods critically depend on inherent redundancy, limiting their applicability as memory optimizations aimed at improving performance and reducing costs (such as Fully Sharded Data Parallelism (FSDP) and ZERO-style optimizations [57–59, 73]) deliberately eliminate this redundancy. Thus, there is a strong need for checkpoint-based techniques that can deliver robust fault tolerance in redundancy-constrained training setups. MoEtion complements redundancy-dependent methods, offering a comprehensive, robust, and efficient checkpoint-based solution tailored specifically for large-scale sparse MoE models, thus ensuring broad applicability across diverse training scenarios.

3 The MOETION Approach

3.1 MOETION Overview

MoEtion is a distributed, in-memory checkpointing system tailored to the expert-parallel architecture of MoE models. It reduces checkpointing overhead by exploiting the skewed and iteration-varying token-to-expert assignment patterns inherent in MoE training, while preserving synchronous training semantics and ensuring fast and accurate failure recovery.

MoEtion introduces three key ideas. First, *Sparse Checkpointing* incrementally captures subsets of modules’ FP32 states across multiple training iterations, rather than checkpointing the full model state simultaneously. By spreading the overhead across a sparse checkpointing window, it achieves negligible runtime overhead during fault-free execution, enabling continuous checkpointing at high frequency. Second, *Sparse-to-Dense Checkpoint Conversion* addresses the temporal inconsistency introduced by sparse snapshots. It incrementally reconstructs a logically consistent dense checkpoint by selectively replaying computations and gradually activat-

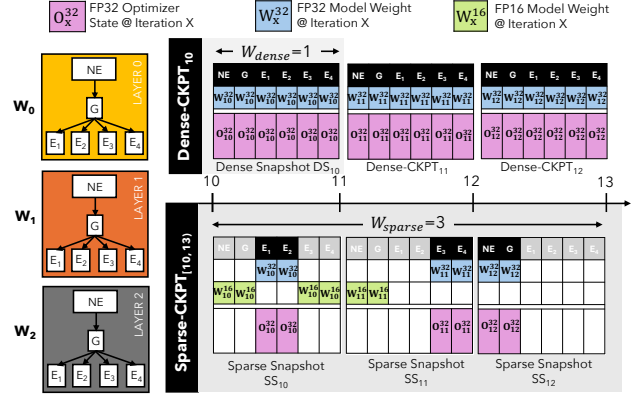


Figure 6: Dense checkpointing simultaneously snapshots FP32 optimizer states and model weights for all modules in one iteration. Sparse checkpointing incrementally snapshots FP32 states of different module subsets across a window of iterations.

ing modules as their full FP32 states become available. This technique ensures correctness and recovery accuracy comparable to traditional dense checkpointing without incurring dense snapshot overhead. Third, *Upstream Activation and Gradient Logging* captures two tensors at each pipeline-stage boundary during training: input activations flowing forward from upstream stages and gradients propagating backward from downstream stages. Logging occurs upstream (at the sender), guaranteeing these tensors remain accessible even if downstream workers fail. During recovery, these logs enable each pipeline stage to independently and precisely recompute the states of workers lost due to failures, without redundant recomputation of unaffected workers. Consequently, recovery is localized exclusively to the impacted data-parallel groups, narrowing the scope and cost of rollback.

Collectively, these techniques decouple runtime overhead from checkpoint completeness, allowing MoEtion to perform high-frequency, stall-free checkpointing with rapid and fully accurate recovery. Table 1 contrasts MoEtion with other state-of-the-art approaches, highlighting its unique ability to simultaneously provide stall-free checkpointing, low overhead at high frequency, fast and fully accurate recovery, and consistently high ETTR. Thus, MoEtion offers robust fault tolerance that is broadly applicable across diverse sparse model sizes, training configurations, and realistic failure scenarios common in large-scale MoE training.

3.2 Avoiding Stalls with Sparse Snapshots

MoEtion exploits two key insights to achieve efficient, stall-free checkpointing. First, expert operators vary significantly in popularity, with some experts being activated far more frequently than others. This imbalance lets us strategically distribute snapshot overhead by checkpointing less popular operators earlier within a sparse checkpoint window. We detail the mechanisms and benefits of this popularity-based operator scheduling in Section 3.5. Second, the iterative structure of training allows reconstructing an operator’s current FP32

state by replaying computations from an earlier snapshot. Thus, rather than checkpointing all modules simultaneously, sparse checkpointing incrementally captures subsets of modules across multiple iterations within a sparse checkpointing window W_{sparse} . At each iteration, only a small subset of operators receives a full FP32 checkpoint (model parameters and optimizer state), significantly reducing the per-iteration snapshot overhead. Operators not yet checkpointed within the current window remain temporarily in a lightweight state, deferring details about how this lightweight state is managed to Section 3.3. Overall, this incremental approach ensures continuous, stall-free checkpointing.

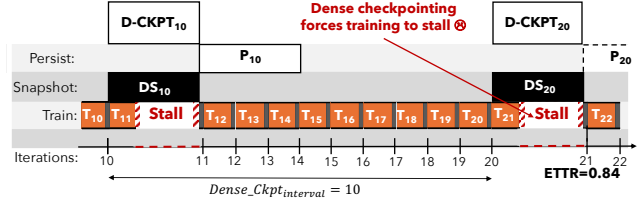
We define a *snapshot* as capturing the model parameters and optimizer states from GPU to local CPU memory during training. Traditional *dense* checkpointing methods snapshot the entire model state simultaneously within a single iteration ($W_{\text{dense}} = 1$). If the dense snapshot operation does not finish before the next optimizer update, training stalls. Figure 7a illustrates this issue: at iteration 11, the snapshot cannot fully overlap with computation, forcing a stall. Thus, dense checkpoints must be infrequent (every 10 iterations in the example) to amortize overhead.

In contrast, sparse checkpointing treats each expert, non-expert, and gating module as independently checkpointable. Each module is checkpointed exactly once within each sparse checkpointing window W_{sparse} , with timing strategically determined by module popularity (discussed further in Section 3.5). Unlike simpler round-robin methods (e.g., MoC-System), MoEtion’s popularity-aware selection minimizes computational overhead during recovery.

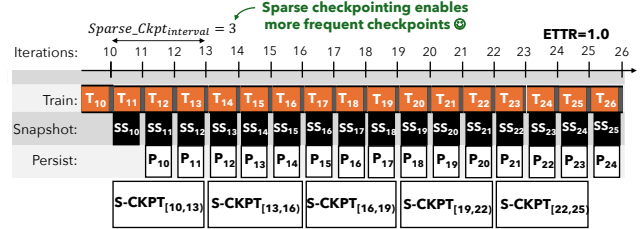
Figure 6 concretely illustrates sparse checkpointing with a three-layer MoE model (each layer has non-expert (NE), gating (G), and four expert modules (E_1 – E_4)). During iteration 11, dense checkpointing (DS_{10}) snapshots all modules simultaneously. Sparse checkpointing (SS_{10}) captures FP32 states only for experts E_1, E_2 . In iteration 12, sparse snapshot (SS_{11}) captures FP32 states for experts E_3, E_4 , and finally, at iteration 13, modules NE, G are checkpointed (SS_{12}). Thus, each module receives exactly one FP32 snapshot within the window.

Figure 7b further demonstrates how sparse checkpointing incrementally snapshots subsets of modules, entirely avoiding stalls and enabling high-frequency checkpointing.

Persisting Snapshots: After capturing a snapshot to local CPU memory, the subsequent *persist* operation—replicating snapshots durably—is performed asynchronously alongside training. Like Gemini, MoEtion asynchronously replicates snapshots to remote CPU memory on r peer nodes (buddies). A sparse checkpoint is considered persisted once all its snapshots within the window W_{sparse} are replicated remotely. MoEtion ensures at least one persisted checkpoint and another checkpoint in-flight at all times. Once a new sparse checkpoint is persisted, the oldest checkpoint is garbage collected.



(a) Dense checkpointing stalls training; checkpoints occur infrequently.



(b) Sparse checkpointing fully overlaps with training, eliminating stalls and enabling frequent checkpoints.

Figure 7: Dense vs. sparse checkpointing timelines.

The Consistency Challenge: Sparse checkpointing avoids stalls but introduces temporal inconsistencies: different modules within one sparse checkpoint window are checkpointed at distinct iterations. For instance, within $S\text{-CKPT}_{[10,13]}$, modules E_1, E_2 are checkpointed at iteration 10, E_3, E_4 at iteration 11, and NE, G at iteration 12. Without resolving these discrepancies, recovery results in incorrect model states, degrading accuracy [16, 46, 54]. Ensuring temporal consistency is thus crucial for accurate fault recovery and reliable debugging.

3.3 Ensuring Correctness with Sparse-to-Dense Checkpoint Conversion

To resolve temporal inconsistencies introduced by sparse checkpointing, MoEtion incrementally reconstructs a logically consistent dense checkpoint from multiple sparse snapshots. We rely on the critical insight that, given a previous complete FP32 snapshot for an operator, its state at the current iteration can be precisely reconstructed by replaying exactly the microbatches it processed since the snapshot. To enable accurate replay and backpropagation, we save these FP16 model weights (2 bytes per parameter) at intermediate iterations for all operators awaiting their full FP32 checkpoints in each sparse snapshot. These FP16 weights are sufficient for forward passes and input-gradient computations during replay, drastically reducing per-iteration snapshot sizes compared to storing full FP32 states (12 bytes per parameter).

When loading a sparse snapshot, each module is classified as either *active* or *frozen* based on the availability of its FP32 optimizer state and FP32 model weights. Active modules possess their complete FP32 states, enabling full participation in forward passes, backward passes, and optimizer updates. Conversely, frozen modules, possessing only FP16 model weights, execute forward passes and backward passes with respect to inputs (B_{input}), but bypass gradient computations with respect to weights (B_{weight}) and the optimizer update

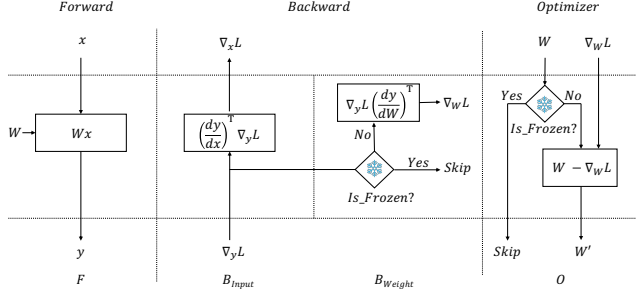


Figure 8: Illustration of forward, backward, and optimizer steps for frozen vs. active operators. Frozen operators compute activations and input gradients but skip weight gradients and optimizer updates, thus maintaining stable FP16 states until their FP32 states become available.

step. Figure 8 illustrates this conditional execution clearly: frozen modules check their activation status before the B_{weight} step and skip expensive gradient computations and updates, whereas active modules proceed normally.

Figure 9 illustrates how MoEtion incrementally reconstructs a dense checkpoint at iteration 13 (D-CKPT₁₃) from sparse snapshots (SS₁₀–SS₁₂), forming the sparse checkpoint window S-CKPT_[10,13], using the MoE layer from Figure 6. Initially, loading snapshot SS₁₀ during iteration 11 activates modules E_1 and E_2 , which have complete FP32 states, while modules E_3 , E_4 , G, and NE remain frozen with FP16 weights only (1). As iteration 11 microbatches are replayed, the active modules (E_1 , E_2) advance their states to iteration 11, updating parameters and optimizer states. Frozen modules propagate activations and gradients without updates (2).

Next, loading snapshot SS₁₁ during iteration 12 activates additional modules E_3 and E_4 alongside E_1 and E_2 , while G and NE remain frozen (3). Replay of iteration 12 updates parameters and optimizer states for active modules (E_1 – E_4), synchronizing them to iteration 12, whereas frozen modules continue propagating gradients without updates (4).

Finally, loading snapshot SS₁₂ during iteration 13 activates the remaining modules G and NE, resulting in all modules (E_1 – E_4 , G, NE) being fully active (5). Replay of iteration 13 synchronizes parameters and optimizer states for all modules, achieving a consistent dense checkpoint state identical to a traditional dense checkpoint taken at iteration 13 (6).

By the end of iteration 13, this staged replay ensures all modules’ parameters and optimizer states precisely match those that would have been obtained using conventional dense checkpointing, achieving correctness without incurring dense checkpoint overhead. Thus, the sparse-to-dense conversion technique enables MoEtion to simultaneously leverage the efficiency of frequent, stall-free sparse checkpoints and the accuracy and consistency advantages of dense checkpointing.

3.4 Minimizing Recomputation with Logging

Checkpoint-based fault tolerance inherently introduces recomputation overhead. Classical checkpointing techniques typi-

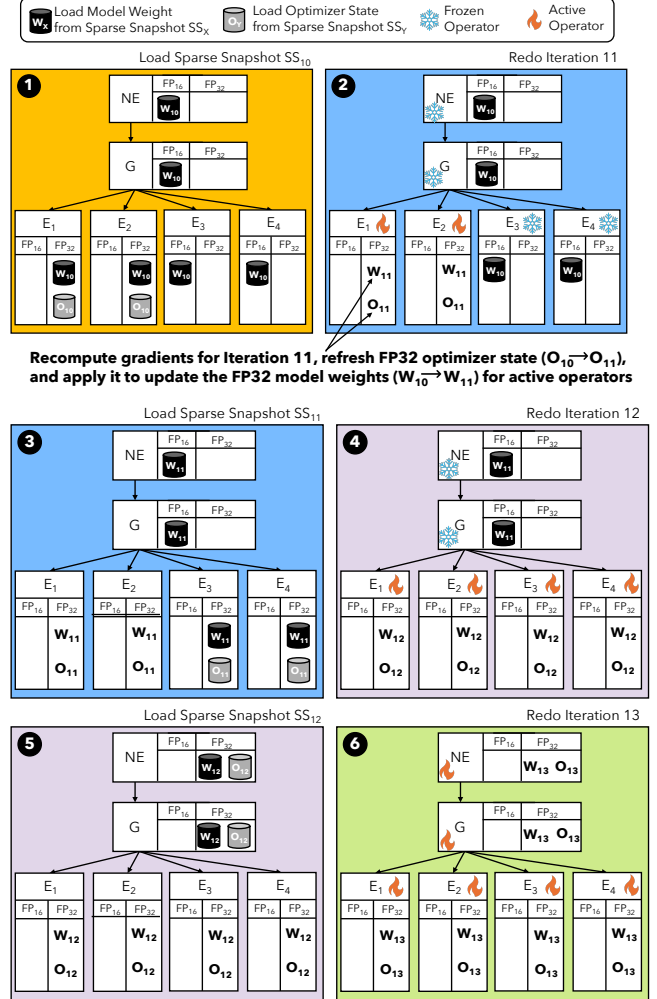


Figure 9: Step-by-step illustration of sparse-to-dense checkpoint conversion over iterations 11–13. Modules incrementally transition from frozen (FP16-only) to fully active (FP32) status as their complete state becomes available from sparse snapshots, allowing them to participate in parameter updates. By iteration 13, a logically consistent dense checkpoint (D-CKPT₁₃) is fully reconstructed from sparse snapshots (SS₁₀–SS₁₂).

cally incur recomputation proportional to half the checkpoint interval. While sparse checkpointing combined with sparse-to-dense conversion significantly reduces runtime overhead, it introduces a new source of recomputation: pipeline stages that lack recent full checkpoints must replay computations to restore consistency. Eliminating this recomputation entirely is difficult. MoEtion drastically reduces its scope through a lightweight logging mechanism that localizes and parallelizes recovery to affected pipeline stages.

Without logging, reconstructing a dense checkpoint from sparse snapshots forces adjacent pipeline stages—even those unaffected by failures—to roll back and recompute the entire sparse checkpoint window (W_{sparse}). This extensive recomputation increases recovery latency, as illustrated in Figure 10

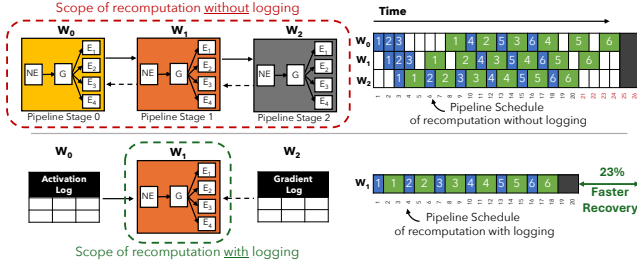


Figure 10: Comparison of recomputation scope and recovery schedule with and without logging. Without logging (top), pipeline stage W_1 's recovery necessitates recomputation across all pipeline stages (W_0 , W_1 , W_2), significantly increasing overhead. With logging (bottom), recomputation is localized exclusively to the affected pipeline stage (W_1), enabling faster and more efficient recovery.

(top). For instance, recovering pipeline stage W_1 would require recomputation across all stages W_0 , W_1 , and W_2 .

To mitigate this overhead, MoEtion incorporates a lightweight logging mechanism designed to localize rollback to only the affected pipeline stages. During forward and backward propagation, MoEtion logs two types of intermediate tensors at each pipeline stage boundary: (1) activations flowing downstream from upstream stages during forward propagation, and (2) gradients flowing upstream from downstream stages during backward propagation. Crucially, logging occurs upstream—i.e., at the sender stage—ensuring logged tensors remain accessible and intact even if downstream stages subsequently fail. Each logged tensor includes metadata, such as iteration numbers and micro-batch identifiers, to enable accurate, ordered replay during recovery.

Upon detecting a failure, the affected pipeline stages leverage these logged activations and gradients to independently reconstruct their internal states without recomputing any upstream computations. Consequently, recomputation efforts are localized exclusively to the failed data-parallel group, substantially reducing both the scope and duration of the recovery process. As depicted in Figure 10 (bottom), when pipeline stage W_1 fails, logging enables recomputation to remain confined entirely within W_1 . This targeted, localized replay significantly reduces recovery latency—in this example, achieving a 23% faster recovery compared to the scenario without logging.

Parallelizing Recovery from Multiple Concurrent Failures. Logging also simplifies parallel recovery when multiple failures occur simultaneously. Since logged tensors enable independent, localized recomputation, multiple pipeline stages or data-parallel groups experiencing concurrent failures can reconstruct their internal states independently and concurrently. This parallelism significantly accelerates overall recovery compared to sequential or globally coordinated rollback strategies, particularly valuable in large-scale deployments where simultaneous failures are more frequent.

Logged tensors from earlier sparse checkpoint windows become obsolete upon successfully completing and replicating new sparse checkpoints, typically every W_{sparse} iterations. MoEtion proactively garbage-collects obsolete logs to maintain controlled and predictable memory usage. Empirically, for the MoE models evaluated in §5.6, logged tensors represent a modest memory overhead—typically less than 5% of the total baseline memory footprint—confirming that the logging overhead is minimal even at large model scales.

3.5 Sparse Checkpointing Policy

To achieve stall-free sparse checkpointing, MoEtion carefully determines the optimal sparse checkpoint window size (W_{sparse})—the number of iterations over which training state is incrementally captured. Smaller windows reduce recomputation after failures but increase runtime overhead, while larger windows lower overhead but lead to longer recomputations.

Critically, in addition to the window size, the checkpointing order of operators significantly impacts recovery efficiency. Operators frequently activated by many tokens ("popular experts") incur higher computational costs when transitioning from lightweight, frozen states to fully active states during recovery. By checkpointing less popular experts first and deferring popular experts until later iterations, MoEtion maximizes the duration that popular experts remain frozen, thereby reducing computational overhead during recovery. Frozen operators require only forward passes and input-gradient backward computations, which are $\approx 33\%$ cheaper than active operators. Consequently, this popularity-based ordering strategy accelerates recovery, particularly benefiting large-scale training environments prone to frequent failures.

Adaptive Ordering Based on Popularity Drift. Since operator popularity shifts dynamically throughout training, MoEtion continuously tracks activation counts for each expert operator. Popularity is defined as the frequency of token activation per operator. Formally, the activation count for expert j in layer l is:

$$a_l^j = \sum_{(x_i, y_i) \in \mathcal{D}} \mathbf{1}[\gamma(e_l^j, x_i) = 1],$$

where $\gamma(e_l^j, x_i)$ indicates whether expert j in layer l is activated for token x_i . Alternatively, a soft-count variant leveraging gating probabilities is also supported:

$$a_l^j = \sum_{(x_i, y_i) \in \mathcal{D}} \text{softmax}(g_l(f_l(x_i)))^j.$$

Algorithm 1 Sparse Checkpoint Scheduling

```
1:  $L \leftarrow$  Number of pipeline layers.
2:  $M[\ell] \leftarrow$  Modules in layer  $\ell$ , sorted by ascending popularity.
3:  $T_{\text{idle}} \leftarrow$  Idle time available per iteration.
4:  $S_{\text{FP32}}(m) \leftarrow$  FP32 model size of module  $m$ .
5:  $S_{\text{FP16}}(m) \leftarrow$  FP16 model size of module  $m$ .
6:  $S_{\text{opt}}(m) \leftarrow$  Optimizer state size of module  $m$ .
7:  $B_{\text{PCIe}} \leftarrow$  Effective GPU-to-CPU bandwidth.
8: procedure CKPTSCHE-
   ULE( $L, M, T_{\text{idle}}, S_{\text{FP32}}, S_{\text{FP16}}, S_{\text{opt}}, B_{\text{PCIe}}$ )
9:    $W_{\text{sparse}} \leftarrow 1$ 
10:  while True do
11:     $S_{\text{iter}} \leftarrow 0$   $\triangleright$  Snapshot size per iteration
12:    for  $\ell \in \{0, \dots, L-1\}$  do
13:       $N \leftarrow |M[\ell]|$ 
14:       $S_{\text{FP32-total}} \leftarrow \sum_{m \in M[\ell]} (S_{\text{FP32}}(m) + S_{\text{opt}}(m))$ 
15:       $S_{\ell} \leftarrow S_{\text{FP32-total}} / W_{\text{sparse}}$ 
16:      for  $i \in \{1, \dots, W_{\text{sparse}} - 1\}$  do
17:         $start \leftarrow i \times N / W_{\text{sparse}} + 1$ 
18:         $M_{\text{FP16}} \leftarrow M[\ell][start : N]$ 
19:         $S_{\ell} += \frac{1}{W_{\text{sparse}}} \sum_{m \in M_{\text{FP16}}} S_{\text{FP16}}(m)$ 
20:      end for
21:       $S_{\text{iter}} += S_{\ell}$ 
22:    end for
23:    if  $S_{\text{iter}} / B_{\text{PCIe}} \leq T_{\text{idle}}$  then
24:      break  $\triangleright$  Found smallest window without stall
25:    end if
26:     $W_{\text{sparse}} += 1$ 
27:  end while
28:   $\mathcal{S} \leftarrow$  empty schedule
29:  for  $\ell \in \{0, \dots, L-1\}$  do
30:     $N \leftarrow |M[\ell]|$ 
31:    for  $i \in \{1, \dots, W_{\text{sparse}}\}$  do
32:       $start \leftarrow (i-1) \times N / W_{\text{sparse}} + 1$ 
33:       $end \leftarrow i \times N / W_{\text{sparse}}$ 
34:       $\mathcal{S}[\ell][i].\text{FP32} \leftarrow M[\ell][start : end]$ 
35:       $\mathcal{S}[\ell][i].\text{FP16} \leftarrow M[\ell][end+1 : N]$ 
36:    end for
37:  end for
38:  return  $W_{\text{sparse}}, \mathcal{S}$ 
39: end procedure
```

MoEtion adaptively recalculates the sparse checkpointing window and operator ordering whenever a significant popularity drift occurs—specifically, if activation counts for at least 25% of expert operators change by more than 10%. This adaptive approach maintains optimal checkpointing efficiency without incurring frequent recalculations.

Determining the Optimal Sparse Checkpoint Window. Algorithm 1 computes the smallest sparse checkpoint window size (W_{sparse}) that ensures the snapshotting overhead fully overlaps with available GPU idle time, thus guaranteeing stall-

Model	#Layers	#Experts Per Layer	Gate	Model Dimension	#Parameters	#Active Parameters
MoE-LLaVa-2.9B/4E [44]	32	4	Top-2	1024	2.9B	2B
GPT-7.3B/32E [56]	12	32	Top-2	1536	7.3B	3.6B
QWen-14.3B/64E [70]	24	64	Top-8	2048	14.3B	2.7B
DeepSeek-16.4B/64E [11]	28	2+62	Top-8	2048	16.4B	2.8B

Table 2: Specifications of models used for evaluation.

free checkpointing. Given expert operators sorted by ascending popularity (least popular first), the algorithm iteratively evaluates increasing window sizes, computing snapshot sizes per iteration, until the checkpoint overhead fits within the idle GPU cycles. The resulting checkpoint schedule specifies precisely which operators’ states (FP32 or FP16) to capture at each iteration, prioritizing less popular operators for earlier snapshotting within the window.

The computational complexity of Algorithm 1 is $O(|L| \cdot |M| \cdot W_{\text{sparse}})$, where $|L|$ denotes layers and $|M|$ denotes the operators per layer. Because recalculations are infrequent and triggered only by significant popularity shifts, the algorithm’s runtime overhead is minimal (≈ 0.1 sec) and executes asynchronously without interrupting ongoing GPU computations.

4 Localized Recovery from Failures

Fast recovery from hardware failures is critical during distributed MoE training to ensure high training efficiency. MoEtion enables fast and localized recovery through *sparse checkpointing*, *upstream logging*, and *sparse-to-dense checkpoint conversion*. The same approach also addresses abnormal training events, such as spikes in the loss function, by selectively rolling back to a known stable state.

When a failure or data anomaly is detected, MoEtion immediately pauses all data-parallel (DP) groups abandoning the current iteration to prevent state inconsistency. The failed node is replaced with a spare. Only the affected DP group rolls back, restoring its most recent sparse checkpoint from local memory or peer nodes, while other groups remain paused with consistent state. Sparse checkpoints capture partial optimizer and weight states across multiple iterations, introducing temporal inconsistencies. Each worker locally replays computations using upstream activation logs and downstream gradient logs, reconstructing a consistent dense checkpoint (D-CKPT₁₆) without requiring global recomputation. Once reconstruction completes, training then resumes synchronously across all DP groups. MoEtion bounds rollback to approximately $\frac{3}{2}W_{\text{sparse}}$ iterations, ensuring minimal disruption.

5 Evaluation

We evaluate the effectiveness of MoEtion in providing efficient and reliable in-memory checkpointing for MoE models. Specifically, we answer the following questions:

- How does MoEtion’s sparse checkpointing impact recovery overhead and training efficiency under controlled, frequent failures? (§5.2)

Model	Checkpointing Interval (iterations)				Avg. Per-Iteration Checkpointing Overhead (seconds, overhead % in parentheses)				MTBF	Total Recovery Time (seconds)				ETTR			
	CheckFreq	Gemini	MoC	MoEtion	CheckFreq	Gemini	MoC	MoEtion		CheckFreq	Gemini	MoC	MoEtion	CheckFreq	Gemini	MoC	MoEtion
MoE-LLaVa-2.9B/4E	57	46	1	1	0.03 (2%)	0.02 (1%)	0.14 (8%)	0.01 (1%)	2H	1265	938	10	11.0	0.945	0.958	0.922	0.981
							2.14 (124%)		1H	2530	1877	20	24.0	0.914	0.935	0.375	0.979
							3.41 (201%)		30M	5059	3754	41	57.0	0.853	0.890	0.328	0.975
							5.39 (318%)		20M	7589	5630	61	74.0	0.792	0.844	0.231	0.971
GPT-7.3B/32E	78	64	1	1	0.03 (1%)	0.03 (1%)	0.18 (9%)	0.03 (1%)	2H	1424	1121	13	18.0	0.937	0.947	0.919	0.979
							3.32 (158%)		1H	2848	2243	25	28.0	0.903	0.919	0.384	0.976
							4.54 (216%)		30M	4486	3840	50	78.0	0.834	0.864	0.326	0.971
							7.90 (376%)		20M	8543	6728	76	105.0	0.765	0.809	0.220	0.966
QWen-14.3B/64E	113	89	1	1	0.05 (2%)	0.04 (2%)	0.19 (9%)	0.04 (2%)	2H	1170	961	15	17.0	0.927	0.934	0.927	0.981
							4.25 (170%)		1H	2340	1920	30	33.0	0.898	0.910	0.380	0.977
							7.10 (284%)		30M	4680	3840	60	83.0	0.841	0.862	0.325	0.970
							9.23 (369%)		20M	7020	5760	90	140.0	0.783	0.814	0.205	0.963
DeepSeek-16.4B/64E	124	92	1	1	0.08 (3%)	0.07 (2%)	0.22 (8%)	0.06 (2%)	2H	992	800	17	22.0	0.902	0.910	0.933	0.975
							5.75 (198%)		1H	1984	1601	35	51.0	0.877	0.889	0.349	0.964
							8.58 (293%)		30M	3967	3202	70	104.0	0.827	0.848	0.324	0.965
							12.87 (444%)		20M	5951	4802	104	267.0	0.777	0.807	0.168	0.956

Table 3: Comparison of checkpointing techniques across representative MoE models under varying MTBF scenarios (2 hours to 20 minutes). We report checkpoint intervals, average per-iteration overhead (percentage overhead relative to fault-free execution in parentheses), total recovery times, and Effective Training Time Ratio (ETTR). Highest ETTR values are highlighted in **boldface**.

- How effective is MoEtion in maintaining high ETTR under real-world failure scenarios from large-scale production environments? (§5.3)
- Does MoEtion ensure accurate state recovery and maintain model accuracy despite frequent interruptions? (§5.4)
- How does each of MoEtion’s core techniques contribute to overall performance improvements? (§5.5)

We show that MoEtion consistently maintains high ETTR, delivers accurate model recovery with no loss in downstream task accuracy, and significantly outperforms state-of-the-art checkpointing systems under both controlled and realistic failure conditions.

5.1 Experimental Setup

Cluster Setup. All of our experiments were conducted on a GPU cluster with 12 Standard_NC96ads_A100_v4 nodes, each of which has a 64-core AMD EPYC 7V13 CPU, 880 GB of RAM, and eight NVIDIA A100 80 GB GPUs on Azure Cloud. GPUs on the same node are connected via a 600 GB/s NVLink interconnect, and nodes are connected via 80 Gbps inter-node interconnect across 8 NICs. Azure Blob Storage is used as the remote persistent storage and the aggregated bandwidth to it is 40Gbps. All servers run 64-bit Ubuntu 22.04 with CUDA library v12.8, and DeepSpeed v0.16.

Baselines. We compare MoEtion against Gemini [68], a state-of-the-art in-memory checkpointing system, CheckFreq [50], a disk-based checkpointing alternative, and MoC-System [8], a recent MoE-specific checkpointing technique. To assess potential interference from these checkpointing systems, we also measured the throughput of DeepSpeed-MoE [59] with checkpointing disabled, utilizing a 1F1B interleaved schedule and ZERO Stage-1 optimizations [57]. All experiments were conducted on the same Azure cluster.

Models. We evaluate all systems using the four representative MoE models shown in Table 2: MoE-LLaVa [44], GPT-MoE [1], QWen-MoE [70], and DeepSeek-MoE [11]. GPT-MoE, QWen-MoE, and DeepSeek-MoE are pre-trained using

parallelization strategies (PP, DP, EP) degrees of (3, 4, 8), (6, 2, 8), and (12, 1, 8) respectively. Pre-Traininig used the RedPajama dataset [69] with a batch size of 512, micro-batch size of 32, and sequence length of 2048 tokens. MoE-LLaVa is pre-trained on the ImageNet-1K dataset [10] using (PP, DP, EP) degrees of (6, 2, 8).

5.2 Training Efficiency Under Controlled Failures

We evaluate the performance of MoEtion under controlled failure conditions using four representative MoE models: MoE-LLaVa-2.9B/4E, GPT-7.3B/32E, QWen-14.3B/64E, and DeepSeek-16.4B/64E. We vary the Mean Time Between Failures (MTBF) from 2 hours down to 20 minutes over a 12-hour long training run, covering realistic failure scenarios encountered in large-scale GPU clusters. Table 3 summarizes our key findings, specifically addressing three questions:

How frequently can each technique checkpoint, and at what overhead? Checkpoint frequency significantly impacts both runtime overhead and recovery performance. CheckFreq and Gemini experience stalls during checkpointing, necessitating longer intervals to amortize overhead effectively. At a high MTBF of 2 hours, CheckFreq checkpoint intervals vary from 57 iterations (MoE-LLaVa-2.9B) to 124 iterations (DeepSeek-16.4B), while Gemini checkpoints more frequently at 46 to 92 iterations, maintaining a consistently low overhead (≤ 0.08 seconds per iteration, $\leq 3\%$).

MoC-System adopts an always-on (every iteration) checkpointing approach, which initially benefits recovery by minimizing recomputation. However, its checkpoint overhead dramatically increases at higher failure frequencies, as the system must checkpoint more experts per iteration to preserve model accuracy. At the lowest MTBF of 20 minutes, MoC’s overhead becomes substantial: 5.39 seconds per iteration (318% overhead over fault-free case) for MoE-LLaVa-2.9B and up to 12.87 seconds per iteration (444%) for DeepSeek-16.4B.

MoEtion also checkpoints every iteration but leverages sparse checkpointing combined with upstream logging to avoid stalls entirely. Consequently, it consistently maintains

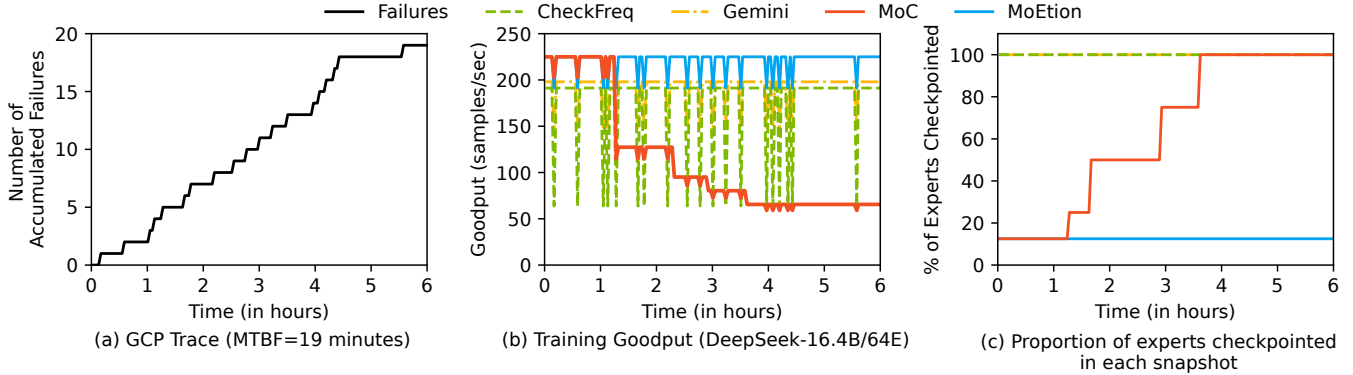


Figure 11: Training goodput (in samples/sec, higher is better) for the DeepSeek-16.4B/64E model over a 6-hour GCP failure trace. (a) Cumulative failures occurring throughout the trace. (b) Throughput comparison: CheckFreq and Gemini show consistently lower throughput due to checkpointing overheads, while MoC-System’s throughput decreases as failures accumulate. MoEtion maintains consistently high throughput due to efficient, stall-free sparse checkpointing. (c) Proportion of experts checkpointed by MoC-System grows significantly as failures occur frequently.

minimal overhead across all models and failure scenarios (≤ 0.06 seconds per iteration, $\leq 2\%$).

How quickly can each technique recover from failures?

Recovery time measures the cumulative downtime from all failures occurring during a 12-hour training run. CheckFreq and Gemini incur substantial recomputation due to their relatively long checkpoint intervals, resulting in high recovery costs under frequent failure scenarios. At an MTBF of 20 minutes, CheckFreq’s recovery times range from 5951 seconds (DeepSeek-16.4B/64E) to 8543 seconds (GPT-7.3B/32E). Similarly, Gemini experiences prolonged recovery times ranging between 4802 seconds (DeepSeek-16.4B/64E) and 6728 seconds (GPT-7.3B/32E).

MoC-System initially benefits from very short recovery times (only 10–17 seconds at an MTBF of 2 hours), as it checkpoints every iteration, minimizing recomputation. Even under frequent failure conditions (MTBF = 20 minutes), MoC maintains relatively low recovery times (61–104 seconds), since recomputation remains limited to a single iteration. However, the efficiency gained through low recovery time is overshadowed by its increased checkpoint overhead, which severely impacts its overall training efficiency (ETTR).

MoEtion consistently achieves minimal recovery times by bounding recomputation within a small sparse checkpoint window. At an MTBF of 2 hours, recovery takes just 11–22 seconds across all models. Even under severe failure conditions (MTBF = 20 minutes), MoEtion maintains low total recovery times ranging from 74 seconds (MoE-LLaVa-2.9B) to just 267 seconds (DeepSeek-16.4B), outperforming CheckFreq and Gemini by $31\times$ and $18\times$ respectively, effectively limiting recomputation without incurring excessive overhead.

What is the overall training efficiency under failures? To holistically evaluate each system, we use the Effective Train-

ing Time Ratio (ETTR), capturing both checkpointing overhead and recovery downtime.

At the high MTBF of 2 hours, CheckFreq and Gemini demonstrate respectable ETTRs between 0.90 and 0.96 across models, benefiting from effective overhead amortization with infrequent checkpointing. However, under more frequent failures (MTBF = 20 minutes), their ETTRs sharply degrade due to significantly increased recomputation times. CheckFreq drops to as low as 0.765 on GPT-7.3B, and Gemini similarly falls to 0.807 on DeepSeek-16.4B. MoC-System faces even more severe ETTR degradation at frequent failure rates due to its high checkpointing overhead. At an MTBF of 20 minutes, MoC-System achieves ETTR values as low as 0.168 for DeepSeek-16.4B due to the overheads of its accuracy-preserving checkpointing.

MoEtion robustly maintains superior ETTR values across all tested scenarios, consistently ranging from 0.956 (DeepSeek-16.4B) to 0.971 (MoE-LLaVa-2.9B) at the lowest MTBF of 20 minutes. By combining stall-free sparse checkpointing with minimal recomputation windows, MoEtion successfully minimizes both checkpoint overhead and recovery downtime even under frequent failures.

5.3 Training Efficiency Under Dynamic Failures

To further evaluate MoEtion under realistic conditions, we replayed a 6-hour trace of failures derived from Google Cloud Platform (GCP) instances previously used by Bamboo [64], Ooblock [33], and ReCycle [18]. Figure 11(a) illustrates the cumulative failures over this period, corresponding to an average MTBF of approximately 19 minutes.

Figure 11(b) compares goodput—defined as useful throughput (batches per second) discounting recomputed batches after failures—for each checkpointing method across the trace. CheckFreq and Gemini maintain consistently lower goodput due to frequent recomputation caused by their relatively

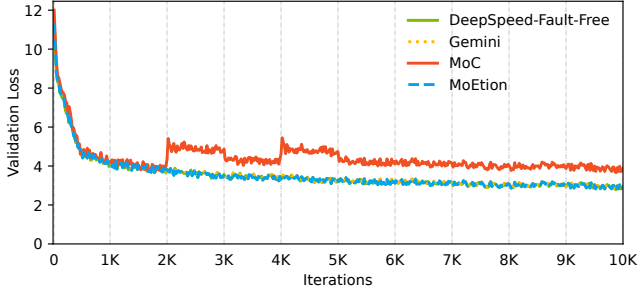


Figure 12: Validation loss of DeepSeek-16.4B/64E model during 10,000 iterations of pretraining, with failures injected at iterations 2,000, 4,000, 6,000, and 8,000 (MTBF \approx 30 minutes).

infrequent checkpointing intervals (124 and 92 iterations, respectively).. MoC-System initially achieves higher goodput due to selectively checkpointing fewer experts. However, as failures accumulate, MoC-System is forced to checkpoint an increasingly larger fraction of experts (Figure 11(c)) to preserve accuracy, leading to significant decreases in goodput over time.

In contrast, MoEtion consistently sustains the highest goodput across the entire duration of the replay, delivering $1.25\times$, $1.15\times$, and $1.98\times$ higher goodput than CheckFreq, Gemini, and MoC-System, respectively. This superior performance highlights MoEtion’s effective balance of minimal recomputation, low overhead, and fast localized recovery under dynamic failure conditions.

5.4 Impact of Failures on Model Accuracy

We next evaluate the impact of checkpointing and recovery mechanisms on model accuracy under failure scenarios. To measure this, we pre-train the DeepSeek-16.4B/64E model for 10,000 iterations, injecting faults at regular intervals (iterations 2,000, 4,000, 6,000, and 8,000), corresponding to an MTBF of approximately 30 minutes. We compare the resulting validation loss trajectories of Gemini, MoC-System, MoEtion, and a fault-free DeepSpeed baseline.

Figure 12 shows that MoC-System exhibits sharp spikes in validation loss immediately following the first two faults (iterations 2,000 and 4,000), due to token loss resulting from incomplete recovery. After iteration 4,000, MoC defaults to checkpointing all experts to mitigate further accuracy degradation, preventing additional spikes, but its validation loss never recovers fully to match fault-free training performance. Gemini and MoEtion closely track the loss trajectory of the DeepSpeed fault-free baseline, demonstrating that both maintain consistent model accuracy despite frequent failures.

To further assess the impact of these checkpointing strategies on model quality, we evaluate downstream performance on several language understanding and knowledge-intensive tasks—PIQA, HellaSwag, TriviaQA, and NaturalQuestions (Table 4). MoEtion consistently matches the fault-free and Gemini baselines, confirming its ability to maintain model accuracy across diverse downstream tasks. Conversely, MoC

Metric	#Shot	DeepSpeed Fault-Free	Gemini	MoEtion	MoC
PIQA (Acc.)	0-shot	72.4	72.5	72.4	61.2
HellaSwag (Acc.)	0-shot	68.9	68.8	68.8	53.1
TriviaQA (EM)	5-shot	54.8	54.6	55.1	37.5
NaturalQuestions (EM)	5-shot	15.3	15.1	15.3	6.3

Table 4: Downstream evaluation comparing fault-free training (DeepSpeed baseline) against Gemini, MoEtion, and MoC across knowledge-intensive and language modeling tasks. **Bold** is best.

shows significant accuracy degradation on all tasks, underscoring the adverse impact of its incomplete recovery strategy and highlighting the importance of preserving synchronous training semantics under failures.

5.5 MoEtion Performance Breakdown

We analyze the incremental contributions of MoEtion’s techniques—*sparse checkpointing*, *popularity-based operator ordering*, *localized recovery*, and *upstream logging*—to its overall efficiency. Figure 13 summarizes these ETTR improvements across three representative models: MoE-LLaVa-2.9B/4E, QWen-14.3B/64E, and DeepSeek-16.4B/64E.

Sparse checkpointing alone provides baseline ETTR improvements (0.37–0.57) by overlapping partial checkpoints with computation. Introducing popularity-based ordering, which prioritizes less frequently activated operators earlier in the sparse checkpointing window, significantly enhances ETTR for models with many experts—such as QWen (64 experts) and DeepSeek (64 experts)—to between 0.63 and 0.71. However, it offers minimal benefits for MoE-LLaVa, which has only 4 experts, due to limited ordering opportunities.

Localized recovery greatly improves ETTR for models with higher data parallelism and fewer pipeline stages. For instance, MoE-LLaVa sees substantial ETTR improvement (0.71 to 0.91) due to localized recovery, as it has multiple data-parallel groups and a shallow 3-stage pipeline, significantly limiting rollback scope. In contrast, localized recovery provides minimal benefit for DeepSeek, which uses expert parallelism with a single data-parallel group (DP degree of 1). Without upstream logging, DeepSeek’s entire 12-stage pipeline must recompute during recovery, limiting ETTR improvements at this stage.

Finally, adding upstream logging consistently yields ETTR improvements across all models. The impact is particularly pronounced for DeepSeek, increasing ETTR from 0.71 to 0.96, since logging eliminates unnecessary recomputation across 11 pipeline stages. For MoE-LLaVa, with fewer pipeline stages, upstream logging still improves ETTR (from 0.91 to 0.97), albeit more modestly.

These results highlight how each technique contributes uniquely and contextually, with sparse checkpointing and upstream logging universally beneficial, popularity ordering impactful for models with many experts, and localized recovery crucial for configurations with substantial data parallelism.

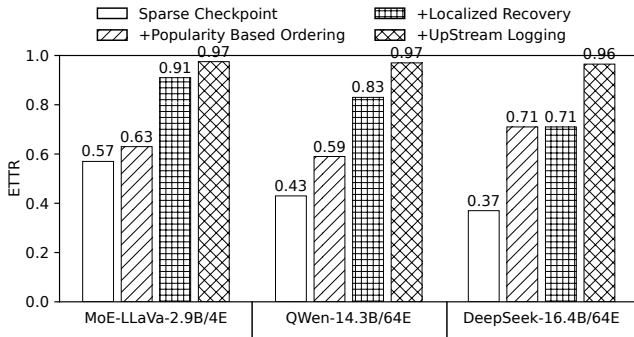


Figure 13: Performance breakdown of MoEtion across three models. Each incremental technique contributes to improving ETTR by reducing recovery overhead, with the full MoEtion stack achieving the highest ETTR.

5.6 Memory Overhead of MoEtion

MoEtion introduces only a modest CPU memory overhead, primarily stemming from storing FP16 snapshots and activation-gradient logs necessary for sparse-to-dense checkpoint conversion and efficient localized recovery. Across the evaluated models (Table 2), this overhead consistently averages around 17% of the total snapshot size per GPU worker. Specifically, approximately 15% arises from holding intermediate FP16 snapshots for operators awaiting their complete FP32 checkpoints, with activation and gradient logs contributing the remaining 2%. Importantly, this modest memory investment allows MoEtion to provide continuous, stall-free checkpointing capabilities without compromising synchronous training semantics.

6 Conclusion

We presented MoEtion, a distributed checkpointing system tailored specifically for efficient and reliable MoE model training. MoEtion introduces three novel techniques—*sparse checkpointing*, *sparse-to-dense checkpoint conversion*, and *lightweight upstream activation and gradient logging*—which collectively address the fundamental runtime–recovery trade-off, correctness–efficiency tension, and excessive global recomputation of existing checkpointing approaches. Our evaluation demonstrates that MoEtion achieves stall-free checkpointing at every iteration, significantly reduces recovery latency, and maintains high Effective Training Time Ratios (ETTR) across diverse failure scenarios. Critically, MoEtion delivers these improvements without sacrificing model accuracy, highlighting its effectiveness as a robust and scalable checkpointing solution for training next-generation foundation models.

References

[1] Josh Achiam, Steven Adler, Sandhini Agarwal, Lama Ahmad, Ilge Akkaya, Florencia Leoni Aleman, Diogo Almeida, Janko Altenschmidt, Sam Altman, Shyamal Anadkat, et al. 2024. GPT-4 Technical Report.

(2024). arXiv:2303.08774 <https://arxiv.org/abs/2303.08774>

- [2] Amey Agrawal, Sameer Reddy, Satwik Bhattamishra, Venkata Prabhakara Sarath Nookala, Vidushi Vashishth, Kexin Rong, and Alexey Tumanov. 2024. Inshrinkerator: Compressing Deep Learning Training Checkpoints via Dynamic Quantization. In *Proceedings of the 2024 ACM Symposium on Cloud Computing (Redmond, WA, USA) (SoCC '24)*. Association for Computing Machinery, New York, NY, USA, 1012–1031. <https://doi.org/10.1145/3698038.3698553>
- [3] Meta AI. 2024. Meta Llama 3. <https://ai.meta.com/blog/meta-llama-3/>.
- [4] Paul Barham, Aakanksha Chowdhery, Jeff Dean, Sanjay Ghemawat, Steven Hand, Dan Hurt, Michael Isard, Hyeontaek Lim, Ruoming Pang, Sudip Roy, Brennan Saeta, Parker Schuh, Ryan Sepassi, Laurent El Shafey, Chandramohan A. Thekkath, and Yonghui Wu. 2022. Pathways: Asynchronous Distributed Dataflow for ML. *arXiv e-prints*, Article arXiv:2203.12533 (March 2022), arXiv:2203.12533 pages. <https://doi.org/10.48550/arXiv.2203.12533> [cs.DC]
- [5] Romain Beaumont. 2022. Large Scale OpenCLIP: L/14, H/14 AND G/14 Trained on LAION-2B. <https://laion.ai/blog/large-openclip/>.
- [6] Tom B. Brown, Benjamin Mann, Nick Ryder, Melanie Subbiah, Jared Kaplan, Prafulla Dhariwal, Arvind Neelakantan, Pranav Shyam, Girish Sastry, Amanda Askell, Sandhini Agarwal, Ariel Herbert-Voss, Gretchen Krueger, Tom Henighan, Rewon Child, Aditya Ramesh, Daniel M. Ziegler, Jeffrey Wu, Clemens Winter, Christopher Hesse, Mark Chen, Eric Sigler, Mateusz Litwin, Scott Gray, Benjamin Chess, Jack Clark, Christopher Berner, Sam McCandlish, Alec Radford, Ilya Sutskever, and Dario Amodei. 2020. Language Models are Few-Shot Learners. *arXiv e-prints*, Article arXiv:2005.14165 (May 2020), arXiv:2005.14165 pages. <https://doi.org/10.48550/arXiv.2005.14165> [cs.CL]
- [7] Weilin Cai, Juyong Jiang, Fan Wang, Jing Tang, Sunghun Kim, and Jiayi Huang. 2025. A Survey on Mixture of Experts in Large Language Models. *IEEE Transactions on Knowledge and Data Engineering* (2025), 1–20. <https://doi.org/10.1109/TKDE.2025.3554028>
- [8] Weilin Cai, Le Qin, and Jiayi Huang. 2025. MoC-System: Efficient Fault Tolerance for Sparse Mixture-of-Experts Model Training. In *Proceedings of the 30th*

ACM International Conference on Architectural Support for Programming Languages and Operating Systems, Volume 2 (Rotterdam, Netherlands) (ASPLOS '25). Association for Computing Machinery, New York, NY, USA, 655–671. <https://doi.org/10.1145/3676641.3716006>

- [9] BLOOM Chronicles. 2022. BLOOM Chronicles. <https://github.com/bigscience-workshop/bigscience/blob/master/train/tr11-176B-ml/chronicles.md>.
- [10] Justin Cui, Ruochen Wang, Si Si, and Cho-Jui Hsieh. 2023. Scaling up dataset distillation to imagenet-1k with constant memory. In *International Conference on Machine Learning*. PMLR, 6565–6590.
- [11] Damai Dai, Chengqi Deng, Chenggang Zhao, RX Xu, Huazuo Gao, Deli Chen, Jiashi Li, Wangding Zeng, Xingkai Yu, Yu Wu, et al. 2024. Deepseekmoe: Towards ultimate expert specialization in mixture-of-experts language models. *arXiv preprint arXiv:2401.06066* (2024).
- [12] John T Daly. 2006. A higher order estimate of the optimum checkpoint interval for restart dumps. *Future generation computer systems* 22, 3 (2006), 303–312.
- [13] Databricks. 2024. Introducing DBRX: A New State-of-the-Art Open LLM. <https://www.databricks.com/blog/introducing-dbrx-new-state-art-open-llm/>.
- [14] Jeffrey Dean and Sanjay Ghemawat. 2004. MapReduce: Simplified Data Processing on Large Clusters. In *6th Symposium on Operating Systems Design & Implementation (OSDI 04)*. USENIX Association, San Francisco, CA. <https://www.usenix.org/conference/osdi-04/mapreduce-simplified-data-processing-large-clusters>
- [15] Nan Du, Yanping Huang, Andrew M. Dai, Simon Tong, Dmitry Lepikhin, Yuanzhong Xu, Maxim Krikun, Yanqi Zhou, Adams Wei Yu, Orhan Firat, Barret Zoph, Liam Fedus, Maarten Bosma, Zongwei Zhou, Tao Wang, Yu Emma Wang, Kellie Webster, Marie Pellat, Kevin Robinson, Kathleen Meier-Hellstern, Toju Duke, Lucas Dixon, Kun Zhang, Quoc V Le, Yonghui Wu, Zhifeng Chen, and Claire Cui. 2022. GLaM: Efficient Scaling of Language Models with Mixture-of-Experts. *arXiv:2112.06905* [cs.CL] <https://arxiv.org/abs/2112.06905>
- [16] Assaf Eisenman, Kiran Kumar Matam, Steven Ingram, Dheevatsa Mudigere, Raghuraman Krishnamoorthi, Krishnakumar Nair, Misha Smelyanskiy, and Murali Annavaram. 2022. Check-N-Run: a Checkpointing System for Training Deep Learning Recommendation Models. In *19th USENIX Symposium on Networked Systems Design and Implementation (NSDI 22)*. USENIX Association, Renton, WA, 929–943. <https://www.usenix.org/conference/nsdi22/presentation/eisenman>
- [17] William Fedus, Barret Zoph, and Noam Shazeer. 2021. Switch Transformers: Scaling to Trillion Parameter Models with Simple and Efficient Sparsity. *arXiv e-prints*, Article arXiv:2101.03961 (Jan. 2021), arXiv:2101.03961 pages. <https://doi.org/10.48550/arXiv.2101.03961> arXiv:2101.03961 [cs.LG]
- [18] Swapnil Gandhi, Mark Zhao, Athinagoras Skiadopoulos, and Christos Kozyrakis. 2024. ReCycle: Resilient Training of Large DNNs using Pipeline Adaptation. In *Proceedings of the ACM SIGOPS 30th Symposium on Operating Systems Principles* (Austin, TX, USA) (SOSP '24). Association for Computing Machinery, New York, NY, USA, 211–228. <https://doi.org/10.1145/3694715.3695960>
- [19] Gemini. 2025. Gemini 2.5: Our most intelligent AI model. <https://blog.google/technology/google-deepmind/gemini-model-thinking-updates-march-2025/>.
- [20] Priya Goyal, Piotr Dollár, Ross Girshick, Pieter Noordhuis, Lukasz Wesolowski, Aapo Kyrola, Andrew Tulloch, Yangqing Jia, and Kaiming He. 2017. Accurate, Large Minibatch SGD: Training ImageNet in 1 Hour. *arXiv e-prints*, Article arXiv:1706.02677 (June 2017), arXiv:1706.02677 pages. <https://doi.org/10.48550/arXiv.1706.02677> arXiv:1706.02677 [cs.CV]
- [21] Daya Guo, Dejian Yang, Haowei Zhang, Junxiao Song, Ruoyu Zhang, Runxin Xu, Qihao Zhu, Shirong Ma, Peiyi Wang, Xiao Bi, et al. 2025. Deepseek-r1: Incentivizing reasoning capability in llms via reinforcement learning. *arXiv preprint arXiv:2501.12948* (2025).
- [22] Saurabh Gupta, Tirthak Patel, Christian Engelmann, and Devesh Tiwari. 2017. Failures in large scale systems: long-term measurement, analysis, and implications. In *Proceedings of the International Conference for High Performance Computing, Networking, Storage and Analysis (SC '17)*. Association for Computing Machinery, New York, NY, USA, Article 44, 12 pages. <https://doi.org/10.1145/3126908.3126937>
- [23] Tanmaey Gupta, Sanjeev Krishnan, Rituraj Kumar, Abhishek Vijeev, Bhargav Gulavani, Nipun Kwatra, Ramachandran Ramjee, and Muthian Sivathanu. 2024. Just-In-Time Checkpointing: Low Cost Error Recovery from Deep Learning Training Failures. In *Proceedings of the Nineteenth European Conference on Computer Systems* (Athens, Greece) (EuroSys '24). Associ-

- ation for Computing Machinery, New York, NY, USA, 1110–1125. <https://doi.org/10.1145/3627703.3650085>
- [24] Ethan He, Abhinav Khattar, Ryan Prenger, Vijay Korthikanti, Zijie Yan, Tong Liu, Shiqing Fan, Ashwath Aithal, Mohammad Shoeybi, and Bryan Catanzaro. 2024. Upcycling large language models into mixture of experts. *arXiv preprint arXiv:2410.07524* (2024).
- [25] Jiaao He, Jiezhong Qiu, Aohan Zeng, Zhilin Yang, Jidong Zhai, and Jie Tang. 2021. Fast-MoE: A Fast Mixture-of-Expert Training System. arXiv:2103.13262 [cs.LG] <https://arxiv.org/abs/2103.13262>
- [26] Jiaao He, Jidong Zhai, Tiago Antunes, Haojie Wang, Fuwen Luo, Shangfeng Shi, and Qin Li. 2022. Faster-MoE: modeling and optimizing training of large-scale dynamic pre-trained models. In *Proceedings of the 27th ACM SIGPLAN Symposium on Principles and Practice of Parallel Programming* (Seoul, Republic of Korea) (PPoPP '22). Association for Computing Machinery, New York, NY, USA, 120–134. <https://doi.org/10.1145/3503221.3508418>
- [27] Tao He, Xue Li, Zhibin Wang, Kun Qian, Jingbo Xu, Wenyuan Yu, and Jingren Zhou. 2023. Unicorn: Economizing Self-Healing LLM Training at Scale. *arXiv e-prints*, Article arXiv:2401.00134 (Dec. 2023), arXiv:2401.00134 pages. <https://doi.org/10.48550/arXiv.2401.00134> arXiv:2401.00134 [cs.DC]
- [28] Xu Owen He. 2024. Mixture of A Million Experts. arXiv:2407.04153 [cs.LG] <https://arxiv.org/abs/2407.04153>
- [29] Jordan Hoffmann, Sebastian Borgeaud, Arthur Mensch, Elena Buchatskaya, Trevor Cai, Eliza Rutherford, Diego de Las Casas, Lisa Anne Hendricks, Johannes Welbl, Aidan Clark, Tom Hennigan, Eric Noland, Katie Millican, George van den Driessche, Bogdan Damoc, Aurelia Guy, Simon Osindero, Karen Simonyan, Erich Elsen, Jack W. Rae, Oriol Vinyals, and Laurent Sifre. 2022. Training Compute-Optimal Large Language Models. *arXiv e-prints*, Article arXiv:2203.15556 (March 2022), arXiv:2203.15556 pages. <https://doi.org/10.48550/arXiv.2203.15556> arXiv:2203.15556 [cs.CL]
- [30] Qinghao Hu, Zhisheng Ye, Zerui Wang, Guoteng Wang, Meng Zhang, Qiaoling Chen, Peng Sun, Dahua Lin, Xiaolin Wang, Yingwei Luo, Yonggang Wen, and Tianwei Zhang. 2024. Characterization of large language model development in the datacenter. In *Proceedings of the 21st USENIX Symposium on Networked Systems Design and Implementation* (Santa Clara, CA, USA) (NSDI'24). USENIX Association, USA, Article 39, 21 pages.
- [31] Yanping Huang, Youlong Cheng, Ankur Bapna, Orhan Firat, Mia Xu Chen, Dehao Chen, Hyoungho Lee, Jiquan Ngiam, Quoc V. Le, Yonghui Wu, and Zhifeng Chen. 2019. *GPipe: efficient training of giant neural networks using pipeline parallelism*. Curran Associates Inc., Red Hook, NY, USA.
- [32] Changho Hwang, Wei Cui, Yifan Xiong, Ziyue Yang, Ze Liu, Han Hu, Zilong Wang, Rafael Salas, Jithin Jose, Prabhat Ram, HoYuen Chau, Peng Cheng, Fan Yang, Mao Yang, and Yongqiang Xiong. 2023. Tutel: Adaptive Mixture-of-Experts at Scale. In *Proceedings of Machine Learning and Systems*, D. Song, M. Carbin, and T. Chen (Eds.), Vol. 5. Curran, 269–287. https://proceedings.mlsys.org/paper_files/paper/2023/file/5616d34cf8ff73942cfd5aa922842556-Paper-mlsys2023.pdf
- [33] Insu Jang, Zhenning Yang, Zhen Zhang, Xin Jin, and Mosharaf Chowdhury. 2023. Ooblock: Resilient Distributed Training of Large Models Using Pipeline Templates. In *Proceedings of the 29th Symposium on Operating Systems Principles (SOSP '23)*. Association for Computing Machinery, New York, NY, USA, 382–395. <https://doi.org/10.1145/3600006.3613152>
- [34] Myeongjae Jeon, Shivaram Venkataraman, Amar Phanishayee, Junjie Qian, Wencong Xiao, and Fan Yang. 2019. Analysis of Large-Scale Multi-Tenant GPU Clusters for DNN Training Workloads. In *2019 USENIX Annual Technical Conference (USENIX ATC 19)*. USENIX Association, Renton, WA, 947–960. <https://www.usenix.org/conference/atc19/presentation/jeon>
- [35] Albert Q. Jiang, Alexandre Sablayrolles, Antoine Roux, Arthur Mensch, Blanche Savary, Chris Bamford, Devendra Singh Chaplot, Diego de las Casas, Emma Bou Hanna, Florian Bressand, Gianna Lengyel, Guillaume Bour, Guillaume Lample, L lio Renard Lavaud, Lucile Saulnier, Marie-Anne Lachaux, Pierre Stock, Sandeep Subramanian, Sophia Yang, Szymon Antoniak, Teven Le Scao, Th ophile Gervet, Thibaut Lavril, Thomas Wang, Timoth e Lacroix, and William El Sayed. 2024. Mixtral of Experts. arXiv:2401.04088 [cs.LG] <https://arxiv.org/abs/2401.04088>
- [36] Ziheng Jiang, Haibin Lin, Yinmin Zhong, Qi Huang, Yangrui Chen, Zhi Zhang, Yanghua Peng, Xiang Li, Cong Xie, Shibiao Nong, Yulu Jia, Sun He, Hongmin Chen, Zhihao Bai, Qi Hou, Shipeng Yan, Ding Zhou, Yiyao Sheng, Zhuo Jiang, Haohan Xu, Hao-ran Wei, Zhang Zhang, Pengfei Nie, Leqi Zou, Sida Zhao, Liang Xiang, Zherui Liu, Zhe Li, Xiaoying Jia,

- Jianxi Ye, Xin Jin, and Xin Liu. 2024. MegaScale: Scaling Large Language Model Training to More Than 10,000 GPUs. In *21st USENIX Symposium on Networked Systems Design and Implementation (NSDI 24)*. USENIX Association, Santa Clara, CA, 745–760. <https://www.usenix.org/conference/nsdi24/presentation/jiang-ziheng>
- [37] Taebum Kim, Hyoungjoo Kim, Gyeong-In Yu, and Byung-Gon Chun. 2023. BPIPE: memory-balanced pipeline parallelism for training large language models. In *Proceedings of the 40th International Conference on Machine Learning (ICML 23)*. JMLR.org, Article 682, 15 pages.
- [38] Apostolos Kokolis, Michael Kuchnik, John Hoffman, Adithya Kumar, Parth Malani, Faye Ma, Zachary DeVito, Shubho Sengupta, Kalyan Saladi, and Carole-Jean Wu. 2024. Revisiting Reliability in Large-Scale Machine Learning Research Clusters. *arXiv preprint arXiv:2410.21680* (2024).
- [39] Jakub Krajewski, Jan Ludziejewski, Kamil Adamczewski, Maciej Pióro, Michał Krutul, Szymon Antoniak, Kamil Ciebiera, Krystian Król, Tomasz Odrzygóźdź, Piotr Sankowski, et al. 2024. Scaling laws for fine-grained mixture of experts. *arXiv preprint arXiv:2402.07871* (2024).
- [40] Teven Le Scao et al. 2022. BLOOM: A 176B-Parameter Open-Access Multilingual Language Model. *arXiv e-prints*, Article arXiv:2211.05100 (Nov. 2022), arXiv:2211.05100 pages. <https://doi.org/10.48550/arXiv.2211.05100> arXiv:2211.05100 [cs.CL]
- [41] Dmitry Lepikhin, HyoukJoong Lee, Yuanzhong Xu, Dehao Chen, Orhan Firat, Yanping Huang, Maxim Krikun, Noam Shazeer, and Zhifeng Chen. 2020. GShard: Scaling Giant Models with Conditional Computation and Automatic Sharding. *arXiv e-prints*, Article arXiv:2006.16668 (June 2020), arXiv:2006.16668 pages. <https://doi.org/10.48550/arXiv.2006.16668> arXiv:2006.16668 [cs.CL]
- [42] Shigang Li and Torsten Hoefler. 2021. Chimera: efficiently training large-scale neural networks with bidirectional pipelines. In *Proceedings of the International Conference for High Performance Computing, Networking, Storage and Analysis (SC '21)*. Association for Computing Machinery, New York, NY, USA, Article 27, 14 pages. <https://doi.org/10.1145/3458817.3476145>
- [43] Shen Li, Yanli Zhao, Rohan Varma, Omkar Salpekar, Pieter Noordhuis, Teng Li, Adam Paszke, Jeff Smith, Brian Vaughan, Pritam Damania, and Soumith Chintala. 2020. PyTorch distributed: experiences on accelerating data parallel training. *Proc. VLDB Endow.* 13, 12 (aug 2020), 3005–3018. <https://doi.org/10.14778/3415478.3415530>
- [44] Bin Lin, Zhenyu Tang, Yang Ye, Jiayi Cui, Bin Zhu, Peng Jin, Jinfa Huang, Junwu Zhang, Yatian Pang, Munnan Ning, et al. 2024. Moe-llava: Mixture of experts for large vision-language models. *arXiv preprint arXiv:2401.15947* (2024).
- [45] Aixian Liu, Bei Feng, Bing Xue, Bingxuan Wang, Bochao Wu, Chengda Lu, Chenggang Zhao, Chengqi Deng, Chenyu Zhang, Chong Ruan, et al. 2024. Deepseek-V3 Technical Report. *arXiv preprint arXiv:2412.19437* (2024). <https://arxiv.org/abs/2412.19437>
- [46] Kiwan Maeng, Shivam Bharuka, Isabel Gao, Mark Jeffrey, Vikram Saraph, Bor-Yiing Su, Caroline Trippel, Jiyan Yang, Mike Rabbat, Brandon Lucia, et al. 2021. Understanding and improving failure tolerant training for deep learning recommendation with partial recovery. *Proceedings of Machine Learning and Systems* 3 (2021), 637–651.
- [47] Avinash Maurya, Robert Underwood, M. Mustafa Rafique, Franck Cappello, and Bogdan Nicolae. 2024. DataStates-LLM: Lazy Asynchronous Checkpointing for Large Language Models. In *Proceedings of the 33rd International Symposium on High-Performance Parallel and Distributed Computing (Pisa, Italy) (HPDC '24)*. Association for Computing Machinery, New York, NY, USA, 227–239. <https://doi.org/10.1145/3625549.3658685>
- [48] Qi Meng, Wei Chen, Yue Wang, Zhi-Ming Ma, and Tie-Yan Liu. 2019. Convergence analysis of distributed stochastic gradient descent with shuffling. *Neurocomputing* 337 (2019), 46–57.
- [49] Meta. 2025. The Llama 4 herd: The beginning of a new era of natively multimodal AI innovation. <https://ai.meta.com/blog/llama-4-multimodal-intelligence/>.
- [50] Jayashree Mohan, Amar Phanishayee, and Vijay Chidambaram. 2021. CheckFreq: Frequent, Fine-Grained DNN Checkpointing. In *19th USENIX Conference on File and Storage Technologies (FAST 21)*. USENIX Association, 203–216. <https://www.usenix.org/conference/fast21/presentation/mohan>
- [51] Deepak Narayanan, Aaron Harlap, Amar Phanishayee, Vivek Seshadri, Nikhil R. Devanur, Gregory R. Ganger, Phillip B. Gibbons, and Matei Zaharia. 2019. PipeDream: generalized pipeline parallelism for DNN

- training. In *Proceedings of the 27th ACM Symposium on Operating Systems Principles (SOSP '19)*. Association for Computing Machinery, New York, NY, USA, 1–15. <https://doi.org/10.1145/3341301.3359646>
- [52] Deepak Narayanan, Mohammad Shoeybi, Jared Casper, Patrick LeGresley, Mostofa Patwary, Vijay Korthikanti, Dmitri Vainbrand, Prethvi Kashinkunti, Julie Bernauer, Bryan Catanzaro, Amar Phanishayee, and Matei Zaharia. 2021. Efficient large-scale language model training on GPU clusters using megatron-LM. In *Proceedings of the International Conference for High Performance Computing, Networking, Storage and Analysis (SC '21)*. Association for Computing Machinery, New York, NY, USA, Article 58, 15 pages. <https://doi.org/10.1145/3458817.3476209>
- [53] Maxim Naumov, John Kim, Dheevatsa Mudigere, Srinivas Sridharan, Xiaodong Wang, Whitney Zhao, Serhat Yilmaz, Changkyu Kim, Hector Yuen, Mustafa Ozdal, Krishnakumar Nair, Isabel Gao, Bor-Yiing Su, Jiyan Yang, and Mikhail Smelyanskiy. 2020. Deep Learning Training in Facebook Data Centers: Design of Scale-up and Scale-out Systems. *arXiv e-prints*, Article arXiv:2003.09518 (March 2020), arXiv:2003.09518 pages. <https://doi.org/10.48550/arXiv.2003.09518> arXiv:2003.09518 [cs.DC]
- [54] Aurick Qiao, Bryon Aragam, Bingjing Zhang, and Eric Xing. 2019. Fault tolerance in iterative-convergent machine learning. In *International Conference on Machine Learning*. PMLR, 5220–5230.
- [55] Zihan Qiu, Zeyu Huang, Bo Zheng, Kaiyue Wen, Zekun Wang, Rui Men, Ivan Titov, Dayiheng Liu, Jingren Zhou, and Junyang Lin. 2025. Demons in the Detail: On Implementing Load Balancing Loss for Training Specialized Mixture-of-Expert Models. *arXiv preprint arXiv:2501.11873* (2025).
- [56] Samyam Rajbhandari, Conglong Li, Zhewei Yao, Minjia Zhang, Reza Yazdani Aminabadi, Ammar Ahmad Awan, Jeff Rasley, and Yuxiong He. 2022. DeepSpeed-MoE: Advancing Mixture-of-Experts Inference and Training to Power Next-Generation AI Scale. arXiv:2201.05596 [cs.LG] <https://arxiv.org/abs/2201.05596>
- [57] Samyam Rajbhandari, Jeff Rasley, Olatunji Ruwase, and Yuxiong He. 2020. ZeRO: memory optimizations toward training trillion parameter models. In *Proceedings of the International Conference for High Performance Computing, Networking, Storage and Analysis (SC '20)*. IEEE Press, Article 20, 16 pages.
- [58] Samyam Rajbhandari, Olatunji Ruwase, Jeff Rasley, Shaden Smith, and Yuxiong He. 2021. ZeRO-infinity: breaking the GPU memory wall for extreme scale deep learning. In *Proceedings of the International Conference for High Performance Computing, Networking, Storage and Analysis (SC '21)*. Association for Computing Machinery, New York, NY, USA, Article 59, 14 pages. <https://doi.org/10.1145/3458817.3476205>
- [59] Jeff Rasley, Samyam Rajbhandari, Olatunji Ruwase, and Yuxiong He. 2020. DeepSpeed: System Optimizations Enable Training Deep Learning Models with Over 100 Billion Parameters. In *Proceedings of the 26th ACM SIGKDD International Conference on Knowledge Discovery & Data Mining (KDD '20)*. Association for Computing Machinery, New York, NY, USA, 3505–3506. <https://doi.org/10.1145/3394486.3406703>
- [60] Alexander Sergeev and Mike Del Balso. 2018. Horovod: fast and easy distributed deep learning in TensorFlow. *arXiv e-prints*, Article arXiv:1802.05799 (Feb. 2018), arXiv:1802.05799 pages. <https://doi.org/10.48550/arXiv.1802.05799> arXiv:1802.05799 [cs.LG]
- [61] Mohammad Shoeybi, Mostofa Patwary, Raul Puri, Patrick LeGresley, Jared Casper, and Bryan Catanzaro. 2019. Megatron-LM: Training Multi-Billion Parameter Language Models Using Model Parallelism. *CoRR* abs/1909.08053 (2019). arXiv:1909.08053 <http://arxiv.org/abs/1909.08053>
- [62] Shaden Smith, Mostofa Patwary, Brandon Norick, Patrick LeGresley, Samyam Rajbhandari, Jared Casper, Zhun Liu, Shrimai Prabhumoye, George Zerveas, Vijay Korthikanti, Elton Zhang, Rewon Child, Reza Yazdani Aminabadi, Julie Bernauer, Xia Song, Mohammad Shoeybi, Yuxiong He, Michael Houston, Saurabh Tiwary, and Bryan Catanzaro. 2022. Using DeepSpeed and Megatron to Train Megatron-Turing NLG 530B, A Large-Scale Generative Language Model. *arXiv e-prints*, Article arXiv:2201.11990 (Jan. 2022), arXiv:2201.11990 pages. <https://doi.org/10.48550/arXiv.2201.11990> arXiv:2201.11990 [cs.CL]
- [63] Foteini Strati, Michal Friedman, and Ana Klimovic. 2025. PCcheck: Persistent Concurrent Checkpointing for ML. In *Proceedings of the 30th ACM International Conference on Architectural Support for Programming Languages and Operating Systems, Volume 1* (Rotterdam, Netherlands) (ASPLOS '25). Association for Computing Machinery, New York, NY, USA, 811–827. <https://doi.org/10.1145/3669940.3707255>
- [64] John Thorpe, Pengzhan Zhao, Jonathan Eyolfson, Yifan Qiao, Zhihao Jia, Minjia Zhang, Ravi Netravali, and Guoqing Harry Xu. 2023. Bamboo: Making Preemptible Instances Resilient for Affordable

- Training of Large DNNs. In *20th USENIX Symposium on Networked Systems Design and Implementation (NSDI 23)*. USENIX Association, Boston, MA, 497–513. <https://www.usenix.org/conference/nsdi23/presentation/thorpe>
- [65] Borui Wan, Mingji Han, Yiyao Sheng, Yanghua Peng, Haibin Lin, Mofan Zhang, Zhichao Lai, Menghan Yu, Junda Zhang, Zuquan Song, Xin Liu, and Chuan Wu. 2024. ByteCheckpoint: A Unified Checkpointing System for Large Foundation Model Development. arXiv:2407.20143 [cs.AI] <https://arxiv.org/abs/2407.20143>
- [66] Guanhua Wang, Olatunji Ruwase, Bing Xie, and Yuxiong He. 2024. FastPersist: Accelerating Model Checkpointing in Deep Learning. arXiv:2406.13768 [cs.DC] <https://arxiv.org/abs/2406.13768>
- [67] Stephanie Wang, John Liagouris, Robert Nishihara, Philipp Moritz, Ujval Misra, Alexey Tumanov, and Ion Stoica. 2019. Lineage stash: fault tolerance off the critical path. In *Proceedings of the 27th ACM Symposium on Operating Systems Principles (SOSP '19)*. Association for Computing Machinery, New York, NY, USA, 338–352. <https://doi.org/10.1145/3341301.3359653>
- [68] Zhuang Wang, Zhen Jia, Shuai Zheng, Zhen Zhang, Xinwei Fu, T. S. Eugene Ng, and Yida Wang. 2023. GEMINI: Fast Failure Recovery in Distributed Training with In-Memory Checkpoints. In *Proceedings of the 29th Symposium on Operating Systems Principles (SOSP '23)*. Association for Computing Machinery, New York, NY, USA, 364–381. <https://doi.org/10.1145/3600006.3613145>
- [69] Maurice Weber, Daniel Fu, Quentin Anthony, Yonatan Oren, Shane Adams, Anton Alexandrov, Xiaozhong Lyu, Huu Nguyen, Xiaozhe Yao, Virginia Adams, et al. [n. d.]. Redpajama: an open dataset for training large language models, 2024. URL <https://arxiv.org/abs/2411.12372> ([n. d.]).
- [70] An Yang, Baosong Yang, Beichen Zhang, Binyuan Hui, Bo Zheng, Bowen Yu, Chengyuan Li, Dayiheng Liu, Fei Huang, Haoran Wei, et al. 2024. Qwen2. 5 technical report. arXiv preprint arXiv:2412.15115 (2024).
- [71] John W Young. 1974. A first order approximation to the optimum checkpoint interval. *Commun. ACM* 17, 9 (1974), 530–531.
- [72] Mingshu Zhai, Jiaao He, Zixuan Ma, Zan Zong, Runqing Zhang, and Jidong Zhai. 2023. Smart-MoE: Efficiently Training Sparsely-Activated Models through Combining Offline and Online Parallelization. In *2023 USENIX Annual Technical Conference (USENIX ATC 23)*. USENIX Association, Boston, MA, 961–975. <https://www.usenix.org/conference/atc23/presentation/zhai>
- [73] Yanli Zhao, Andrew Gu, Rohan Varma, Liang Luo, Chien-Chin Huang, Min Xu, Less Wright, Hamid Shojanazeri, Myle Ott, Sam Shleifer, Alban Desmaison, Can Balioglu, Pritam Damania, Bernard Nguyen, Geeta Chauhan, Yuchen Hao, Ajit Mathews, and Shen Li. 2023. PyTorch FSDP: Experiences on Scaling Fully Sharded Data Parallel. *arXiv e-prints*, Article arXiv:2304.11277 (April 2023), arXiv:2304.11277 pages. <https://doi.org/10.48550/arXiv.2304.11277> arXiv:2304.11277 [cs.DC]
- [74] Barret Zoph, Irwan Bello, Sameer Kumar, Nan Du, Yanping Huang, Jeff Dean, Noam Shazeer, and William Fedus. 2022. St-moe: Designing stable and transferable sparse expert models. *arXiv preprint arXiv:2202.08906* (2022).
- [75] Yazhou Zu, Alireza Ghaffarkhah, Hoang-Vu Dang, Brian Towles, Steven Hand, Safeen Huda, Adekunle Bello, Alexander Kolbasov, Arash Rezaei, Dayou Du, Steve Lacy, Hang Wang, Aaron Wisner, Chris Lewis, and Henri Bahini. 2024. Resiliency at Scale: Managing Google’s TPUv4 Machine Learning Supercomputer. In *21st USENIX Symposium on Networked Systems Design and Implementation (NSDI 24)*. USENIX Association, Santa Clara, CA, 761–774. <https://www.usenix.org/conference/nsdi24/presentation/zu>